Assessment of A New Fine-Resolution Nighttime Light Imagery from the Yangwang-1 ("Look Up 1") Satellite

Xiaolin Zhu, *member*, *IEEE*, Xiaoyue Tan, Minglei Liao, Tianshu Liu, Meng Su, Shuheng Zhao, Yi Nam Xu, Xintao Liu

Abstract—**High-resolution nighttime light (NTL) satellite images are needed for monitoring human activities and socioeconomic dynamics at fine scales, but such NTL data is very limited. On 11th June 2021, China launched the Yangwang-1 ("Look Up 1") satellite, which is a small optical space telescope that detects near-Earth asteroids, but its visible band sensor can also collect nighttime light images. It provides a new fine-scale NTL data source. This study assessed the quality and capability of Yangwang-1 NTL imagery for capturing artificial lights. The results show that Yangwang-1 has equivalent quality with the state of the art in the NTL remote sensing (e.g., VIIRS, Luojia-1) and some aspects are even better. Specifically, Yangwang-1 has a higher spatial resolution (40 meters at the nadir), high radiometric consistency with VIIRS (R^2=0.83), higher sensitivity to low lights than Luojia-1, better image quality in the spatial domain (lower BRISQUE index than Luojia-1 and VIIRS by 32% and 61% respectively), and a 420-700 nm broad band that can better detect artificial light and is less influenced by the absorption of the atmosphere. Yangwang-1 NTL data can be applied to various fields, including urban mapping, road network extraction, disaster detection, monitoring light pollution, illegal fishing, fires, and human settlements and mapping associated energy infrastructures at fine scales.**

Index Terms—**Artificial light, fine scale, human activities, nighttime light, Yangwang-1.**

I. INTRODUCTION

Remote sensing of night-time lights (NTL) offers a unique ability to monitor human activities and the urban economy from space [1]. Since the 1990s, many studies have taken advantage of the DMSP/OLS sensor to monitor artificial lights from space and quantify the relationships with socioeconomic variables [2]–[6]. However, these DMSP/OLS-based applications are restricted to a rather coarse spatial and temporal resolution because the nighttime visible band has a spatial resolution above 2.2 km (at nadir) [2] and only the annual composites of DMSP/OLS NTL data are free-access [7], [8]. In the last decade, new avenues have opened to advance the study of NTL remote sensing with the availability of new sensors, offering better spatial, temporal, and radiometric resolution than DMSP/OLS. For example, launched in October 2011, the VIIRS/DNB was designed to collect high-quality radiometric data at the daily frequency with a spatial resolution of 742 m, showing a remarkable capability of NTL observations [7], [9]–[11]. In addition, CubeSats and commercial satellites have recently been launched to provide valuable NTL observations at even higher resolutions. In 2017, a new Chinese satellite, Jilin-1, was launched that can offer NTL data with very high resolution (0.89 m) [12], [13]. As a CubeSat, the Luojia-1 launched in 2018 can offer a global high-precision and free of charge NTL observation with a spatial resolution of 130 m every 15 days [14]. These new satellites have significantly promoted the applications of NTL data, such as mapping urbanization processes, estimating GDP and poverty at fine scales, and estimating nighttime atmospheric conditions [1]. However, Luojia-1 is an experimental satellite with a life expectancy of less than 1 year. Therefore, new satellites with the capacity of observing artificial lights at fine scales are needed to provide timely observations of the artificial light changes associated with human activities.

On 11th June 2021, Origin Space Ltd., a space recourse utilization firm in China, launched the Yangwang-1 ("Look Up 1") satellite, which is a small optical space telescope that uses visible and ultraviolet observations to detect near-Earth asteroids. However, this satellite can spot more than the asteroids. For example, it can capture footage of the aurora australis and meteors as they strike the Earth's atmosphere. Besides, it can collect the nighttime light images by tuning its camera to target the ground. The visible band of Yangwang-1 has a wavelength between 420 to 700 nm which is different from that of VIIRS/DNB and Luojia-1. It collects nighttime imagery with a ground spatial resolution of around 40 m at the nadir. More detailed satellite parameters of Yangwang-1 are summarized in Table I.

Xiaolin Zhu, Minglei Liao, Xiaoyue Tan, Shuheng Zhao, Yi Nam Xu and Xintao Liu are with the Department of Land Surveying and Geo-Informatics, The Hong Kong Polytechnic University, Hong Kong 999077, China

(e-mail: xiaolin.zhu@polyu.edu.hk; minglei.liao@connect.polyu.hk; xiaoyue.tan@connect.polyu.hk; shuheng.zhao@connect.polyu.hk; yi-nam.xu@connect.polyu.hk; xintao.liu@polyu.edu.hk).

Tianshu Liu is with the S.T.E.M Academy, Orange Lutheran High School, Orange, CA 92867, USA (e-mail: 81liutianshu@gmail.com)

Meng Su is with the Laboratory for Space Research, The University of Hong Kong, Hong Kong 999077, China (e-mail: mengsu84@hku.hk).
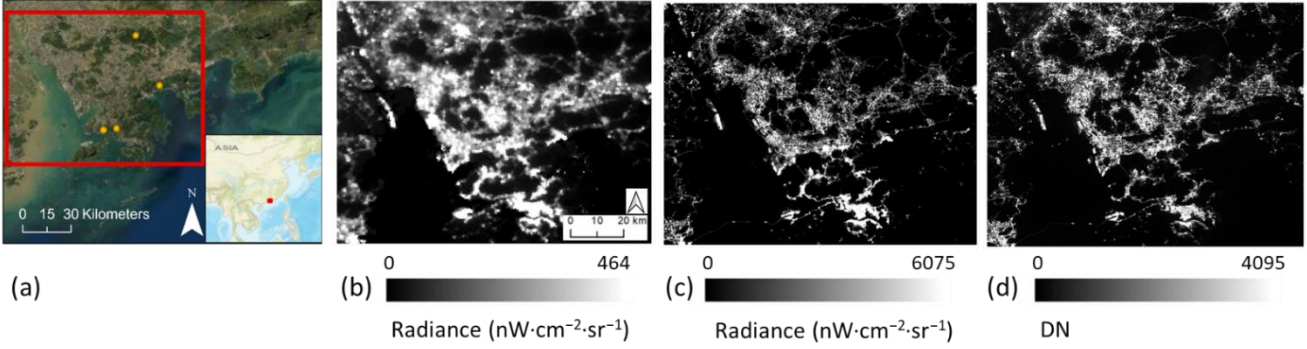
Fig. 1. (a) Position (highlighted in the red point in the lower right map) and the extent of the study area (red box on a true-color satellite image), the yellow points are places used to examine satellites' ability to detect weak light emission. The night-time light images from three sources: (b) VIIRS; (c) Luojia-1; (d) Yangwang-1.

TABLE I
YANGWANG-1 SATELLITE PARAMETERS

Parameter	Value/description
Orbit type	Sun-synchronous orbit
Orbit height	645 km
Optical detector	Temperature-controlled scientific Complementary Metal-Oxide-Semiconductor (sCMOS)
Camera pixel size	2048×2048
Ground sampling swath	$78\ km \times 78\ km$ (nadir viewing)
Exposure time	5 ms – 20 ms (Controlled by ground commands)
Dynamic Range	0.763 nW cm^{-2} sr^{-1} - 329 nW cm^{-2} sr^{-1} (Under exposure time of 10 ms)
Geolocation accuracy	148 m (Star-based calibration)

TABLE II
THE CHARACTERISTICS OF THE THREE NTL DATA IN COMPARISON

Feature	Yangwang-1	Luojia-1	VIIRS
Acquisition date	30th August 2021	3rd September 2018	30th August 2021
Spatial resolution	60m (off-nadir)	130m	750m
Spectral wavelength	420-700 nm	460-980 nm	500-900 nm
Radiometric bits	12	15	16
Passing time (UTC)	14:50	14:44	17:30
Passing time (Local)	22:50	22:44	01:30

II. STUDY AREA AND DATA

The NTL image collected by Yangwang-1 over Greater Bay Area in China was provided by the Origin Space Company, the owner of this new satellite, for analysis [Fig. 1(c)]. Greater Bay Area [Fig. 1(a)] is the largest and most populated urban area and is among the four largest bay areas in the world. It has mixed land use, including built-up surfaces, roads, vegetation, and crops, which makes the nighttime light source heterogeneous. Therefore, it is an ideal region to evaluate the properties of NTL images from the Yangwang-1 satellite. The off-nadir image from Yangwang-1 was taken at 22:50 local time (UTC 14:50) on 30th August, 2021. The weather at the acquisition time was generally clear without clouds and heavy aerosols. However, it is visible that some parts of the images were affected by light hazes. The raw image is projected with the equatorial coordinate system. It was co-registered to the Luojia-1 NTL image with a geographic coordinate system by the manual selection of ground control points and the polynomial method (accuracy: one pixel). The pixel values are digital numbers ranging from 0 to 4095 (i.e., 12 bits).

The benchmark datasets used in this study include NTL images from VIIRS/DNB [Fig. 1(b)] and Luojia-1 [Fig. 1(c)] covering the study area. The basic characteristics of these three NTL datasets were summarized in Table II. NTL images from VIIRS and Luojia-1 were resampled to the spatial resolution of Yangwang-1 for the overlap analysis.

Moonlight and atmosphere-corrected VIIRS NTL images on 30th August 2021 were downloaded from NASA Black Marble dataset (https://blackmarble.gsfc.nasa.gov) [15]. The Luojia-1 image on 3rd September 2018 was selected because Luojia-1 has stopped collecting data. 3rd September 2018 is the closest date to 30th August 2021 among all the available Luojia-1 data in 2018. Although the three-year gap may introduce uncertainties in the comparison between Luojia-1 and Yangwang-1 NTL data, the study area has not experienced large disturbances so that the majority of pixels between Luojia-1 and Yangwang-1 are comparable. The Luojia-1 images were downloaded from its official data platform (http://59.175.109.173:8888/app/login_en.html). The DN values of the Luojia-1 image were converted to radiance using the following equation provided by the metadata:

$$r = 10^{-10} \times DN^{\frac{3}{2}} \times w \qquad (2)$$

where w is the bandwidth 5.21×10^{-7} m.

District-level population data in Shenzhen and Hong Kong in 2020 were obtained from China's national census report and Hong Kong population and household statistics, which were used to test the capability of NTL images in estimating socio-economic parameters.

III. ASSESSMENT RESULTS

A. Radiometric Properties

We first evaluated the radiometric properties of three night-time satellites from two perspectives: (1) the radiometric consistency between Yangwang-1 and the other two sensors, and (2) the radiometric range. For the radiometric consistency, linear regression models were built between the DN values of Yangwang-1 and VIIRS [Fig. 2(a)], as well as between Yangwang-1 and Luojia-1 [Fig. 2(b)] after all images were upscaled to 1.2 km to reduce the impact of geo-registration errors among the three images. The results show that the two linear regression models are very similar (slope 0.051 vs 0.054), but the relationship between Yangwang-1 and VIIRS is stronger than that between Yangwang-1 and Luojia-1 (R^2 0.83 vs 0.68). A possible reason is that Yangwang-1 and VIIRS images both were collected in 2021, but the Luojia-1 image was collected in 2018 that considerable city light changes may have taken place between 2018 and 2021. Since Yangwang-1 has no official calibration equation, the linear regression model between Yangwang-1 and VIIRS was used to calibrate the DN values of Yangwang-1 to radiance for the rest of the analyses in this study. It should be noted that the calibrated radiance of Yangwang-1 may be lower than the actual radiance due to the difference in spectral response between VIIRS and Yangwang-1 (detailed explanation in Section C). In addition, VIIRS passes Hong Kong at 1:30 in local time, however, Yangwang-1 and Luojia-1 pass Hong Kong at 22:50 and 22:44 when there are more lights related to human activities can be detected from space, which should lead to higher NTL radiance [14].

For the radiometric range, Yangwang-1 has the lowest bits compared to VIIRS and Luojia-1 (12 vs 16 and 15) (Table I). We notice that Yangwang-1 has a saturation problem in very bright areas. There is a considerable number of pixels with the maximum digital number (i.e., 4095), corresponding to the most electrified areas, which may result from the limited dynamic range similar to the saturation problem of DMSP [16].

The calibrated radiance of Yangwang-1 was used to estimate the population in 27 districts of Hong Kong and Shenzhen by a linear regression model (Fig. 3). The good performance of this model (r-squared = 0.94) suggests that radiance data obtained by Yangwang-1 is capable of evaluating socio-economic parameters.
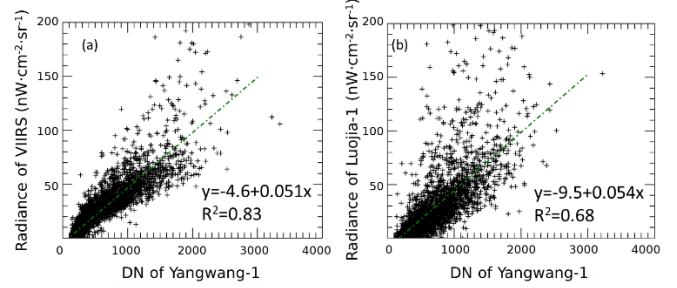

Fig. 2. The linear regression model between Yangwang-1 and (a) VIIRS and (b) Luojia-1.
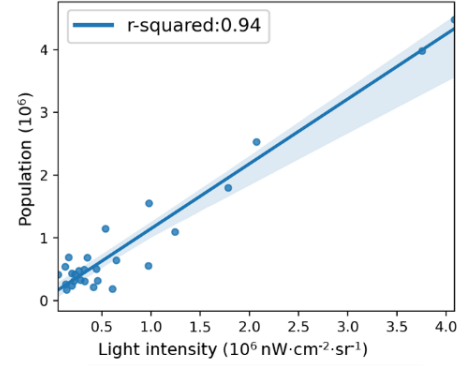

Fig. 3. The linear regression model between the light intensity (obtained by Yangwang-1) and population.

B. Spatial Properties

Among three satellites, Yangwang-1 has the highest spatial resolution about 40 m, which is higher than 130 m of Luojia-1 and dramatically higher than 750 m of VIIRS (Table I). As a result, Yangwang-1 should be more capable to capture the spatial pattern of artificial lights, such as bright city blocks (e.g., business districts) and road networks. To investigate the spatial properties of NTL images from different satellites, a sub-region covering the Hong Kong–Zhuhai–Macau Bridge (HZMB) was selected to demonstrate the NTL spatial patterns (Fig. 4). It is clear that all three satellites can capture the general spatial pattern of NTL, but Yangwang-1 and Luojia-1 NTL images show much more spatial details than VIIRS image. For example, the images from Luojia-1 and Yangwang-1 can clearly capture the Hong Kong–Zhuhai–Macau Bridge (HZMB) (bright line in the middle of Fig. 4(c) and (d)), and the regular shape of the Hong Kong International Airport (the bright patch on the right side of Fig. 4(c) and (d)), but VIIRS cannot spot the HZMB and the image hardly show the shape of the airport [Fig. 4(b)]. The comparison between Yangwang-1 and Luojia-1 in the zoomed area shows that Yangwang-1 [Fig. 4(h)] captures the road network more clearly than Luojia-1 [Fig. 4(g)]. To quantify the image quality in the spatial domain, the dubbed blind/referenceless image spatial quality evaluator (BRISQUE) index [17] was calculated for the three NTL images using a python package (https://pypi.org/project/image-quality/). BRISQUE quantifies losses of "naturalness" in the image due to distortions and a lower value indicates better image quality. To exclude the impact of the saturation problem of Yangwang-1 on the BRISQUE calculation, pixels in all three images with

radiance higher than the saturated value were adjusted to the saturated one and max-min normalization was applied to all images. The results show that Yangwang-1 has a BRISQUE value lower than Luojia-1 and VIIRS (27.4 vs 40.3 and 69.7), indicating that Yangwang-1 has spatial quality better than Luojia-1 and VIIRS by 32% and 61% respectively.

To further quantify the spatial properties, we estimated the spatial response of Luojia-1 and Yangwang-1 using the Hong Kong–Zhuhai–Macau Bridge as ground reference samples. Spatial response refers to the satellite's ability to position ground targets accurately and precisely. The HZMB comprises a 22.9 km-long bridge and a 6.7 km-long Subsea Tunnel connected by two Artificial Islands. In order to provide illumination, the lighting provisions on the HZMB include lights outlining the boundary of the Artificial Islands, street and traffic sign lights, high mast lights, etc. Since the bridge has a width of 33.1 m which is smaller than a pixel of all three satellites, it is ideal to test whether the NTL image is sharp enough to delineate the actual location of the bridge. A transect crossing the bridge was used to investigate the spatial response (Fig. 5). It shows that both Luojia-1 and Yangwang-1 have a peak in NTL that corresponds to the bridge, but the peak of Yangwang-1 has a narrower width than Luojia-1, indicating its superiority in detecting tiny light sources. As for VIIRS, the light is nearly invisible due to the coarse spatial resolution [Fig. 4(b)], so the profile of VIIRS is not included in Fig. 5. In addition, the comparison also indicates that Yangwang-1 is more sensitive than Luojia-1 to low lights (e.g., reflected moonlight or weak emissions), since Yangwang-1 recorded more valid radiance on both sides of the bridge than Luojia-1 (Fig. 5). Further comparisons were conducted on selected sites located in the mountainous areas around cities (yellow points in Fig. 1(a)). As shown in Table III, Yangwang-1 and VIIRS/DNB have similar radiances with a difference of less than 1 nW cm-2 sr-1, whereas Luojia-1 did not record these low radiance values.
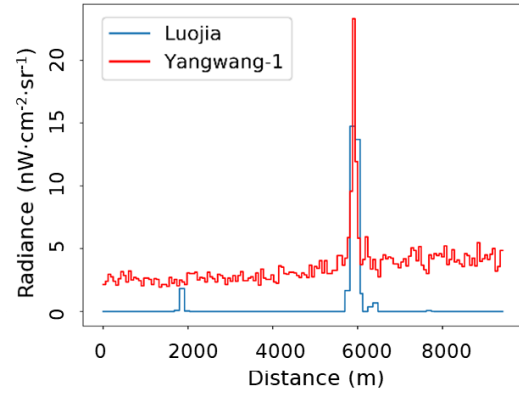
Fig. 5. The NTL profiles of Hong Kong-Zhuhai-Macao Bridge in Fig. 4(d) from Yangwang-1 and Luojia-1.

Table III.
OBSERVED RADIANCE FROM VIIRS, LUOJIA-1, AND YANGWANG-1 IN SELECTED PLACES WITH WEAK LIGHT EMISSION.

Point coordinates	VIIRS	Luojia-1	Yangwang-1
114.17 °E 22.90 °N	4.0	0.0	4.0
114.32 °E 22.63 °N	4.0	0.0	4.8
114.15 °E 22.40 °N	4.9	0.0	4.1
114.04 °E 22.39 °N	4.0	0.0	3.4

C. Spectral Properties

Fig. 6(a) shows the spectral responses of the three satellites for the NTL visible band. Spectral response describes the sensitivity of the sensor to optical radiation of different wavelengths. This is important because spectral responses determine which part of the optical radiation spectrum is measured. The spectral responses of Luojia-1 and VIIRS were collected from previous studies [14], [18]. The spectral response of Yangwang-1 was estimated as the product of the Quantum Efficiency (QE) and lens transmittance data provided by the Yangwang-1 satellite team [19]. Fig. 5 suggests that the spectral response of Yangwang-1 is significantly different from Luojia-1 and VIIRS. It shifts more to the shorter wavelengths, which indicates that Yangwang-1 has some strengths in artificial light monitoring. First, the absorption of the atmosphere mainly happens in the band greater than 650 nm, and Yangwang-1 concentrates on a shorter wavelength ranging from 420 nm to approximately 700 nm, so Yangwang-1 will be less influenced by the absorption of the atmosphere. Second, the energy of three main types of artificial lights (fluorescent, high-pressure sodium, and LED) mainly distributes within the spectral response curve of Yangwang-1 except for the narrow peak of high-pressure sodium (Fig. 6(b)). Therefore, Yangwang-1 is more suitable to be utilized for observing artificial lights, especially for LEDs of which the first peak of energy is out of the spectral responses of Luojia-1 and VIIRS.
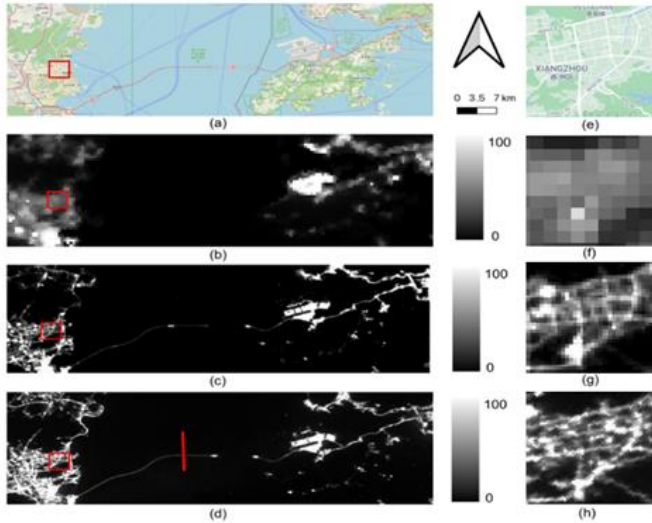

Fig. 4. (a) Google map, (b) VIIRS, (c) Luojia-1, and (d) Yangwang-1 NTL images covering Hong Kong-Zhuhai-Macao Bridge area. (e)-(h) are zoomed images of the red box in (a)-(d). The red line represents the transect used for analyzing spatial response as shown in Fig. 5.
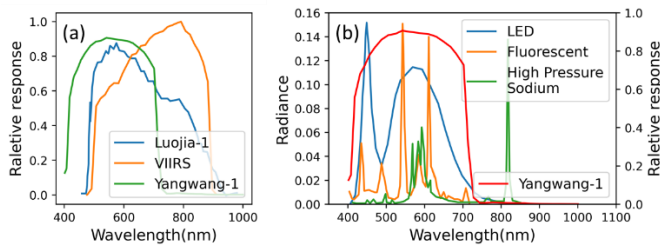
Fig. 6. (a) Three spectral responses for Yangwang-1, Luojia-1, VIIRS. (b) Yangwang-1 spectral response (red line) overlaid with the emission spectra of commonly used city lamps: high-pressure sodium lamp (HPS, green line), fluorescent tube (yellow line), and natural-white LED streetlight lamp (blue line). Note: the unit of lamp radiance is $nWm^{-2}sr^{-1}nm^{-1}$.

IV. DISCUSSIONS AND CONCLUSION

From our assessment, NTL imagery from Yangwang-1 has acceptable quality compared to the state of the art in the NTL remote sensing (e.g., VIIRS, Luojia-1) and some aspects are even better. For the radiometric property, Yangwang-1 has a detectable minimum radiance lower than the other two satellites, so it can better capture weak light emissions. For spatial properties, Yangwang-1 images have the highest spatial resolution among the currently available NTL satellites except for some images acquired through aerial photography and commercial satellites. Therefore, Yangwang-1 can help monitor human activities and socioeconomic disturbances at fine scales, such as neighborhood scale. For spectral property, based on the comparison of spectral response curves, Yangwang-1 is more suitable to detect artificial light and less influenced by the absorption of the atmosphere. Considering the capability and improvement of Yangwang-1 in NTL imaging, Yangwang-1 NTL data can be applied to various fields, including urban mapping, road network extraction, light pollution, illegal fishing, fires, disaster detection, and human settlements and associated energy infrastructures mapping at fine scales. The sample data used in this study can be downloaded from: https://github.com/XZhu-lab/Yangwang-1-NTL-data-assessment.

Although Yangwang-1 images have made remarkable improvements, there are also several limitations. First, it has a saturation problem in very bright areas which may result from the limited dynamic range similar to the saturation problem of DMSP. This issue could be partially mitigated by changing the exposure time. Second, it does not have radiometric calibration parameters to convert the DN values to radiance, thus some quantitative applications may be restricted. Third, considering that the geographic coordinate system is widely used in night-time light, transforming the celestial coordinate system of raw data into commonly used geographic coordinate systems may bring more convenience to end-users. Thus, we suggest the Original Space address the above limitations when releasing the NTL data or developing the next satellites.

REFERENCES

[1] N. Levin *et al.*, "Remote sensing of night lights: A review and an outlook for the future," *Remote Sens. Environ.*, vol. 237, no. October 2018, p. 111443, Feb. 2020, doi: 10.1016/j.rse.2019.111443.

[2] C. D. Elvidge, K. E. Baugh, E. A. Kihn, H. W. Kroehl, and E. R. Davis, "Mapping city lights with nighttime data from the DMSP Operational Linescan System," *Photogrammetric Engineering and Remote Sensing*, vol. 63, no. 6. pp. 727–734, 1997.

[3] M. M. Bennett and L. C. Smith, "Advances in using multitemporal night-time lights satellite imagery to detect, estimate, and monitor socioeconomic dynamics," *Remote Sens. Environ.*, vol. 192, pp. 176–197, 2017, doi: 10.1016/j.rse.2017.01.005.

[4] L. Zhuo, T. Ichinose, J. Zheng, J. Chen, P. J. Shi, and X. Li, "Modelling the population density of China at the pixel level based on DMSP/OLS non-radiance-calibrated night-time light images," *Int. J. Remote Sens.*, vol. 30, no. 4, pp. 1003–1018, Feb. 2009, doi: 10.1080/01431160802430693.

[5] Y. Zhou *et al.*, "A global map of urban extent from nightlights," *Environ. Res. Lett.*, vol. 10, no. 5, May 2015, doi: 10.1088/1748-9326/10/5/054011.

[6] Zhao *et al.*, "Applications of Satellite Remote Sensing of Nighttime Light Observations: Advances, Challenges, and Perspectives," *Remote Sens.*, vol. 11, no. 17, p. 1971, 2019, doi: 10.3390/rs11171971.

[7] C. D. Elvidge, K. E. Baugh, M. Zhizhin, and F.-C. Hsu, "Why VIIRS data are superior to DMSP for mapping nighttime lights," *Proc. Asia-Pacific Adv. Netw.*, vol. 35, no. 0, p. 62, 2013, doi: 10.7125/apan.35.7.

[8] C. D. Elvidge, M. Zhizhin, T. Ghosh, F. C. Hsu, and J. Taneja, "Annual time series of global viirs nighttime lights derived from monthly averages: 2012 to 2019," *Remote Sens.*, vol. 13, no. 5, pp. 1–14, 2021, doi: 10.3390/rs13050922.

[9] S. D. Miller *et al.*, "Illuminating the capabilities of the suomi national Polar-orbiting partnership (NPP) visible infrared imaging radiometer suite (VIIRS) day/night Band," *Remote Sens.*, vol. 5, no. 12, pp. 6717–6766, 2013, doi: 10.3390/rs5126717.

[10] C. D. Elvidge, K. Baugh, M. Zhizhin, F. C. Hsu, and T. Ghosh, "VIIRS night-time lights," *Int. J. Remote Sens.*, vol. 38, no. 21, pp. 5860–5879, 2017, doi: 10.1080/01431161.2017.1342050.

[11] C. C. M. Kyba *et al.*, "High-resolution imagery of earth at night: New sources, opportunities and challenges," *Remote Sens.*, vol. 7, no. 1, pp. 1–23, 2015, doi: 10.3390/rs70100001.

[12] E. Guk and N. Levin, "Analyzing spatial variability in night-time lights using a high spatial resolution color Jilin-1 image – Jerusalem as a case study," *ISPRS J. Photogramm. Remote Sens.*, vol. 163, pp. 121–136, 2020, doi: https://doi.org/10.1016/j.isprsjprs.2020.02.016.

[13] Q. Zheng *et al.*, "A new source of multi-spectral high spatial resolution night-time light imagery — JL1-3B," *Remote Sens. Environ.*, vol. 215, no. October 2017, pp. 300–312, 2018, doi: https://doi.org/10.1016/j.rse.2018.06.016.

[14] X. Li, X. Li, D. Li, X. He, and M. Jendryke, "A preliminary investigation of Luojia-1 night-time light imagery," *Remote Sens. Lett.*, vol. 10, no. 6, pp. 526–535, Jun. 2019, doi: 10.1080/2150704X.2019.1577573.

[15] M. O. Román *et al.*, "NASA's Black Marble nighttime lights product suite," *Remote Sens. Environ.*, vol. 210, no. March, pp. 113–143, Jun. 2018, doi: 10.1016/j.rse.2018.03.017.

[16] H. Letu, M. Hara, G. Tana, and F. Nishio, "A saturated light correction method for DMSP/OLS nighttime satellite imagery," *IEEE Trans. Geosci. Remote Sens.*, vol. 50, no. 2, pp. 389–396, Feb. 2012, doi: 10.1109/TGRS.2011.2178031.

[17] A. Mittal, A. K. Moorthy, and A. C. Bovik, "No-Reference Image Quality Assessment in the Spatial Domain," vol. 21, no. 12, pp. 4695–4708, 2012.

[18] J. Wang *et al.*, "Development of a nighttime shortwave radiative transfer model for remote sensing of nocturnal aerosols and fires from VIIRS," *Remote Sens. Environ.*, vol. 241, no. July 2019, p. 111727, 2020, doi: 10.1016/j.rse.2020.111727.

[19] A. Krishnamurthy, J. Villasenor, S. Seager, G. Ricker, and R. Vanderspek, "Precision characterization of the TESS CCD detectors: Quantum efficiency, charge blooming and undershoot effects," *Acta Astronaut.*, vol. 160, pp. 46–55, 2019, doi: https://doi.org/10.1016/j.actaastro.2019.04.016.